Toxicology Reports 13 (2024) 101698

Contents lists available at ScienceDirect

Toxicology Reports

journal homepage: www.elsevier.com/locate/toxrep

Hesperetin-7-O-rhamnoglucoside ameliorates dichlorvos-facilitated cardiotoxicity in rats by counteracting ionoregulatory, ion pumps, redox, and lipid homeostasis disruptions

Adio J. Akamo [a,b,*], Adetutu O. Ojelabi [b], Oluwatobi T. Somade [b,**], Iyabode A. Kehinde [c], Adewale M. Taiwo [d], Boluwatife A. Olagunju [b], Mushafau A. Akinsanya [a], Adebisi A. Adebisi [a], Tobi S. Adekunbi [a], Abiola F. Adenowo [a], Florence Anifowose [a], Olufemi M. Ajagun-Ogunleye [a], Ofem E. Eteng [b], Jacob K. Akintunde [b], Regina N. Ugbaja [b]

[a] Department of Medical Biochemistry, Faculty of Basic Medical Sciences, Lagos State University College of Medicine, Ikeja, Lagos State, Nigeria
[b] Clinical Biochemistry and Mechanistic Toxicology Research Cluster, Department of Biochemistry, Federal University of Agriculture, Abeokuta, Ogun State, Nigeria
[c] Department of Pure and Applied Botany, Federal University of Agriculture, Abeokuta, Ogun State, Nigeria
[d] Department of Environmental Management and Toxicology, Federal University of Agriculture, Abeokuta, Ogun State, Nigeria

ARTICLE INFO

Handling Editor: Prof. L.H. Lash

Keywords:
Dichlorvos
Hesperetin-7-O-rhamnoglucoside
Cardiotoxicity
Electrolyte
Ion pumps
Redox status
Lipid

ABSTRACT

The contamination of edible agricultural goods with pesticides, including dichlorvos (DVDP), poses a substantial public health risk, promoting severe morbidity and mortality, especially in developing countries. It has been shown that hesperidin (hesperetin-7-O-rhamnoglucoside or Hes-7-RGlc) preserves cytomembrane, redox, and lipid homeostasis; unfortunately, its function on dichlorvos-incited heart damage has not been investigated. This work explored the ameliorative influence of Hes-7-RGlc on DVDP-activated cardiotoxicity. For this end, forty-two rats were randomly appropriated into seven groups (6 rats/group): Control, DVDP alone (8 mg.kg^{-1}day^{-1}), DVDP supplied with either Hes-7-RGlc (50 and 100 mg.kg^{-1}day^{-1}) or the reference medication atropine (0.2 mg.kg^{-1}day^{-1}), and Hes-7-RGlc alone (50 and 10 mg.kg^{-1}day^{-1}) were the seven groups investigated. DVDP was administered orally for seven days, followed by fourteen days of Hes-7-RGlc therapy. Then the rats were euthanized, and their blood and hearts were removed. Hes-7-RGlc chemotherapy substantially ($p<0.05$) restored DVDP-elicited dynamics in plasma and cardiac/myocardium creatine kinase isoenzyme (CK-MB), major lipids (cholesterol, triacylglycerol, and phospholipids), electrolytes (Na^+, K^+, Ca^{2+}, Mg^{2+}, Cl^-), and total protein. Hes-7-RGlc remedy decidedly ($p<0.05$) abolished DDVP-stimulated amplification in the cardiac concentration of H_2O_2, NO and malondialdehyde; annulled DVDP-educed decreases in heart GSH levels, activities of GST, SOD, catalase, and glutathione peroxidase, ion transporters (Na^+/K^+-ATPase and Ca^{2+}/Mg^{2+}-ATPase), ALT, AST, ALP, and LDH-1. Collectively, Hes-7-RGlc can be advocated as a natural supplementary candidate and blocker of DVDP-provoked heart deficits via its capacity to reverse disruptions of electrolytes, ion pumps, redox status, and lipid homeostasis.

1. Introduction

Dichlorvos (2, 2-dichlorovinyl dimethyl phosphate, DDVP) is an alkenyl phosphate, synthetic and broad spectrum fast-acting biocidal pesticide produced from the dehydrochlorination of trichlorfon or the reaction of trimethyl phosphate with chloral [1]. Although it has been outlawed in most European Union (EU) member states and the United Kingdom and restricted in the USA, Canada, Australia, and Korea, it remains the most prevalent organophosphate (OP) insecticide in low- and medium income nations. There, it is used to mitigate pests in agricultural settings, as a household insecticide, antihelminthic (on dogs, horses, and swine), and the elimination of crustacean ectoparasites in

* Corresponding author at: Department of Medical Biochemistry, Faculty of Basic Medical Sciences, Lagos State University College of Medicine, Ikeja, Lagos State, Nigeria.
** Corresponding author.
E-mail addresses: akamoaj@funaab.edu.ng (A.J. Akamo), somadeot@funaab.edu.ng (O.T. Somade).

https://doi.org/10.1016/j.toxrep.2024.101698
Received 27 June 2024; Received in revised form 15 July 2024; Accepted 16 July 2024
Available online 19 July 2024

fish husbandry [2,3]. Dichlorvos has been used for over six decades [2]. Its routes of exposure include inhalation from hazardous waste sites or after pesticide application, and contact with contaminated soil, surfaces and food [4,5].

Dichlorvos degrades quickly in humid air, water, and soil via abiotic and biotic mechanisms. It is abiotically hydrolyzed to dichloroacetaldehyde and dimethylphosphate. Dichloroacetaldehyde is then converted to dichloroethanol, dichloroacetic acid, and CO_2. Dimethylphosphate is converted to methylphosphate, then broken down into phosphate [2]. DDVP is unique among OPs in its fast catabolism and excretion by animals. Despite exposure to 17 times the residential pest control dose, DDVP was not detectable in mice, rats, or humans' blood. Additionally, DDVP does not accumulate in human tissues or cow or rat milk, even at poisoning dosages. This quick elimination is attributable to tissue and blood plasma degrading enzymes [6,7]. In mammals, DDVP is primarily degraded via the liver, though the blood, kidney, lung, and spleen also convert dichlorvos to dimethyl phosphate [2]. This process involves two enzymatic mechanisms: the glutathione-independent mechanism catalyzed by "A" type esterases that is similar to abiotic hydrolysis and the glutathione-dependent mechanism via glutathione S-transferase [8,9].

On a global scale, millions of cases of OP poisonings are recorded annually, with causes ranging from agricultural usage to accidental exposure, suicide attempts, and, in rare cases, homicide [10]. DDVP is swiftly absorbed by the gut and lungs, metabolized in the liver, and excreted through the kidneys. Both acute and chronic exposure to DDVP can result in various visceral injuries, including hepatotoxicity [11], nephrotoxicity [12], hematotoxicity [13], cardiotoxicity [14], neurotoxicity [15], and impaired pancreatic endocrine function leading to diabetes [16].

DDVP-mediated visceral toxicity arises through several pathways, primarily the inhibition of acetylcholinesterase action. While slight inhibition of AChE can enhance cognitive function, as seen in Alzheimer's disease management, excessive inhibition leads to heightened stimulation of cholinergic receptors, eliciting prolonged muscle contraction and excessive salivation, tear production, urination, defecation, gastrointestinal cramping, vomiting, bronchoconstriction, bradycardia, and ultimately respiratory catastrophe. Furthermore, DDVP metabolism in the liver elevates reactive metabolites, depleting the body's antioxidant system, promoting oxidative stress, and impairing cellular processes like apoptosis and ATP synthesis [11–16].

Compounds capable of stabilizing these reactive metabolites, quenching free radicals and abating ionoregulatory, ion pumps, redox, and lipid homeostasis disruptions hold promise in counteracting the deleterious effects of DDVP. Hesperidin (hesperetin-7-O-rhamnoglucoside or Hes-7-RGlc) is a natural bioflavonoid phytochemical primarily found in citrus fruits, including oranges, lemons, and grapefruits, and secondarily in the fabaceae family [17,18]. Hes-7-RGlc is present in various plant components such as fruits, vegetables, nuts, seeds, leaves, flowers, and bark [19]. It has been reported to mitigates various organotoxicities, including nephrocardiotoxicity [20], pulmohepatotoxicity [17,21], neurotoxicity and parotid toxicity [18], via its strong antioxidant, anti-inflammatory, anti-dyslipidemia propensities. Significant factors influencing the impact of Hes-7-RGlc include intestinal flora transformations, absorption and bioavailability [22].

Despite the myriads of protective and antidotal effects of Hes-7-RGlc in reversing xenobiotic-triggered organotoxicity, its ameliorative influence in DDVP-instigated cardiotoxicity has not been elucidated. We postulate that Hes-7-RGlc could quench free radicals and abate ionoregulatory, ion pumps, redox, and lipid homeostasis disruptions. Herein, we explored the chemotherapeutic efficacy of Hes-7-RGlc on DVDP-occasioned cardiotoxicity rat model.

2. Materials and methods

2.1. Chemicals and reagents

O,O-dimethyl-O-(2,2-dichlorovinyl) phosphate ester (DDVP, $C_4H_7Cl_2O_4P$, CAS No. 62–73–7), hesperetin-7-O-rhamnoglucoside ($C_{28}H_{34}O_{15}$, Cat No. SH8070), ketamine hydrochloride ($C_{13}H_{17}Cl_2NO$, CAS No. 1867–66–9), xylazine hydrochloride ($C_{12}H_{17}ClN_2S$, CAS No. 23076–35–9), total protein kit (TP, Randox, Cat. No. TP 245), alanine aminotransferase kit (ALT, Randox, Cat. No. AL 1200), aspartate aminotransferase kit (AST, Randox, Cat. No. AS 1202), alkaline phosphatase kit (ALP, Randox, Cat. No. AP 542), lactate dehydrogenase kit (LDH, BioSystems, COD 12580), creatine kinase-MB kit (CK-MB, Biosystems, COD 12566), sodium kit (Na, Teco, Stock Code: S600–50), potassium kit (K, Teco, Stock Code: P605–50), calcium kit (Ca, Randox, Cat. No. CA 590), magnesium kit (Mg, Biosystems, COD 11797), chloride kit (Cl^-, Teco, Stock Code: C501–480), bicarbonate / total CO_2 kit (HCO_3^-, Gesan, Ref 1500520), triacylglycerol kit (TAG, Labkit, Ref. 30360), cholesterol kit (CHOL, Labkit, Ref. 30180), phospholipids kit (PLs, Labkit, Ref. 30320), bischofite ($MgCl_2 \bullet 6\ H_2O$, CAS No. 7791–18–6), monosodium chloride (NaCl, CAS No. 7647–14–5), monopotassium chloride (KCl, CAS No. 7447–40–7), trizma-base ($C_4H_{11}NO_3$ CAS No. 77–86–1), muriatic acid (HCl, CAS No. 7647–01–0), ATP disodium salt (5′-ATP-Na_2, $C_{10}H_{14}N_5O_{13}P_3 \cdot 2Na$, CAS. No. 987–65–5), G-Strophanthin ($C_{29}H_{44}O_{12}$, CAS. No. 11018–89–6), 2,2,2-trichloroacetic acid (TCA, Cl_3CCOOH, CAS No. 76–03–9), calcium chloride anhydrous ($CaCl_2$, CAS No. 10043–52–4), heparin ($C_{26}H_{42}N_2O_{37}S_5$, CAS No. 9041–08–1), manganese chloride ($MnCl_2$, CAS No. 244589), formyl trichloride ($CHCl_3$, CAS No. 67–66–3), methylol (CH_3OH, CAS No. CAS No.: 67–56–1), potassium dihydrogen phosphate anhydrous (KH_2PO_4, CAS No. 7778–77–0), dipotassium hydrogen phosphate anhydrous (K_2HPO_4, CAS No. 7758–11–4), potassium iodide (KI, CAS No. 7681–11–0), dihydrogen dioxide (H_2O_2, CAS No. 7722–84–1), 4-sulphanilic acid ($NH_2C_6H_4SO_3H$, CAS No. 121–57–3), O-phosphoric acid (H_3PO_4, CAS No. 7664–38–2), 1,2-Ethanediamine, N-1-naphthalenyl-, dihydrochloride ($C_{12}H_{16}Cl_2N_2$, CAS No. 1465–25–4), reduced glutathione (GSH, $CH(CH_2SH)CONHCH_2CO_2H$, CAS No. 70–18–8), 3-Carboxy-4-nitrophenyl disulfide {DTNB, [$-SC_6H_3(NO_2)CO_2H]_2$, CAS No. 69–78–3}, 2,4-Dinitro-1-chlorobenzene (DNCB, $C_6H_3Cl(NO_2)_2$, CAS No. 97–00–7), 2,3-dihydroxyphenol ($C_6H_6O_3$, CAS No. 87–66–1), titriplex [$\{(HOOCCH_2)_2NCH_2\}_2$, CAS No. 60–00–4], ammonium O-molybdate [$(NH_4)_2MoO_4$, CAS No. 13106–76–8], natriumazide (NaN_3, CAS No. 26628–22–8), 4,6-dihydroxy-2-thiopyrimidine ($C_4H_4N_2O_2S$, CAS No. 504–17–6). Chemelex S.A. Diagnostics (Nave J 08420 Canovelles Barcelona) delivered LABKITS. Italy's Gesan Production in Campobello di Mazara supplied the Gesan kits. Randox Laboratories Limited, located in Crumlin, County Antrim, Britain, was connected to order all the Randox kits. Teco kits were procured from Teco Diagnostics in Anaheim, CA 92807, USA. The Biosystems kits were manufactured by Biosystems Diagnostics (Carrer de la Costa Brava, Barcelona, Spain). The source of Hes-7-RGlc was Solarbio Science and Technology Company Limited (Tongzhou District, Beijing, China). St. Louis, MO 63118, US-based Sigma-Aldrich Chemical Co. furnished all additional compounds. All compounds engaged in this exploration were of pure and analytical grade.

2.2. Animal treatments

The forty-two male Wistar rats (12 weeks old, 176–190 g) procured from the College of Biosciences, Federal University of Agriculture, Abeokuta (FUNAAB), were recruited for this undertaking. The rats were lodged in well-aired hanging plastic cages with ample aspen chippings for bedding in a temperature-guarded (29 ± 2°C) and humidity-regulated (49 ± 3 %) location, with a classical 12-hour light: 12-hour dark rhythm. The rats were nourished with a conventional rodent diet and an uncontaminated drinking water source without fetters. Before

beginning the experiments, seven days were spent adapting each animal to its new environment. Every one of the animals got affectionate treatment predicted on the ethos specified by the FUNAAB Ethical Committee and the Animal Research: Reports of In vivo Experiments [23]. The institution accepted the investigational protocol and assigned the researcher with FUNAAB/COLBIOS/BCH/PG/17/0544.

2.3. Experimental strategy

Forty-two acclimatized rats were randomly divided into seven groups: Control, DVDP alone (8 $mg.kg^{-1}day^{-1}$), DVDP supplied with either Hes-7-RGlc (50 and 100 $mg.kg^{-1}day^{-1}$) or the reference medication atropine (0.2 $mg.kg^{-1}day^{-1}$), and Hes-7-RGlc alone (50 and 100 $mg.kg^{-1}day^{-1}$) were the seven groups investigated. DVDP was administered by oral gavage for seven days, followed by fourteen days of Hes-7-RGlc therapy. Then, the rats were euthanized, and their blood and hearts were removed. Dosing occurred between 8 and 9 a.m. The decision to treat the rat with 50 and 100 $mg•kg^{-1}$ of propitious Hes-7-RGlc and 8 $mg•kg^{-1}$ of DDVP, which is one-tenth of oral LD50, was based on the findings of a preceding study [15,24,25]. Furthermore, sub-acute treatment durations (7 days for DDVP and 14 days for Hes-7-RGlc dissolved in olive oil) were chosen based on previous studies [15,24,25]. Below is a description of the setup for the experiment.

- Control group (n = 6): The rat was given distilled water (2 mL/kg) for seven straight days, then olive oil (2 mL/kg) orally for an extra fourteen straight days.
- DDVP alone group (n = 6): The rat was challenged with dichlorvos (8 $mg•kg^{-1}$) orally for seven straight days, then olive oil (2 mL/kg) for an extra fourteen straight days.
- DDVP + atropine group (n = 6): The rat was challenged with dichlorvos (8 $mg•kg^{-1}$) for seven straight days, then atropine (0.2 $mg•kg^{-1}$) for an extra fourteen straight days.
- DDVP + Hes-7-RGlc-50 group (n = 6): The rat was challenged with dichlorvos (8 $mg•kg^{-1}$) for seven straight days, then Hes-7-RGlc (50 $mg•kg^{-1}$) for an extra fourteen straight days.
- DDVP + Hes-7-RGlc-100 group (n = 6): The rat was challenged with dichlorvos (8 $mg•kg^{-1}$) for seven straight days, then Hes-7-RGlc (100 $mg•kg^{-1}$) for an extra fourteen straight days.
- Hes-7-RGlc-50 alone group (n = 6): The rat was given distilled water (2 mL/kg) for seven straight days, then Hes-7-RGlc (50 $mg•kg^{-1}$) for an extra fourteen straight days.
- Hes-7-RGlc-100 alone group (n = 6): The rat was given distilled water (2 mL/kg) for seven straight days, then Hes-7-RGlc (100 $mg•kg^{-1}$) for an extra fourteen straight days.

2.4. Sample (blood and heart) collection and processing systems

The rats were given DDVP for seven and/or Hes-7-RGlc for additional fourteen days; 24 h after the last exposure (day 22), rats were anesthetized interperitoneally with ketamine (100 $mg•kg^{-1}$) and xylazine (10 $mg•kg^{-1}$) as pronounced by Wellington et al. [26]. Their blood was collected via retro-orbital sinus into 10 mL lithium heparinized vials. The plasma was taken out by centrifuging the bottles for 15 minutes at 3000 g while keeping the ambient temperature (30 ± 2°C) and maintained at −20°C for biochemical markers. The rats were then compassionately sacrificed by cervical displacement. The heart was removed and cleaned from adhering tissues and blood stains using ice-cold potassium chloride solution (1.15 %), blotted dry with filter paper, and weighed. A segment (0.4 g) of the heart tissue was homogenized in 3.6 mL of potassium phosphate solution (0.1 M, pH 7.4, 2°C) i.e. (10 % w/v) to produce 10 % homogenate and spun for 15 min at 10, 000 x g to get hepatocyte homogenate's supernatant. The supernatant was extracted at 4°C and stored at −20°C for biochemical biomarkers. At the same time, a tiny part of the heart was also well-maintained in 100 μL of TRIzol and stored at −80°C for mRNA gene expression studies.

2.5. Biochemical assays

The intensity of a particular chromophoric product at a particular wavelength was monitored spectrophotometrically for all experiments.

2.5.1. Total protein level (TPL) assay

Cupric sulphate and protein integrate to induce a cupric-protein or biuret complex in an alkaline medium ($CuSO_4$ + protein → Cu^{2+}-protein complex). According to the manufacturer's pedagogy for the Randox diagnostic kit, the TPL is precisely proportionate to the intensity of the purple/violet colored complex that results [27].

2.5.2. Cytodamage biomarkers enzymes

The ALT, AST, ALP, LDH, and CK-MB activities in plasma and heart homogenate were determined following the protocols outlined in the Randox/biosystem kits guide [28].

ALT transforms L-alanine to pyruvate (L-alanine + 2-oxoglutarate ↔ pyruvate + L-glutamate). Pyruvate oxidizes NADH to NAD^+ (pyruvate + NADH + H+ ↔ lactate + NAD^+). The intensity of color via NADH depletion is proportional to ALT enzymatic efficacy at 340 nm.

AST interconverts L-aspartate and oxaloacetate (L-aspartate + 2-oxoglutarate ↔ oxaloacetate + L-glutamate). Oxaloacetate transforms NADH to NAD^+ (oxaloacetate + NADH + H+ ↔ malate + NAD^+). The AST enzyme kinetics is correlated with the decrease in optical density at 340 nm.

At a pH > 9, ALP degrades p-nitrophenyl phosphate (PNPP) to p-nitrophenol, an intense yellow chromogenic compound [PNPP + H_2O → Pi + PNP]. The rise in the substrate's luminosity associates with ALP catalytic activity at 405 nm.

LDH reversibly converts pyruvate to lactate (pyruvate + NADH ↔ lactate + NAD^+). The degree of rise in absorbance at 340 nm as NADH depletes indicates LDH enzymatic function.

CK transfers phosphate group from creatine phosphate to ADP (creatine-P + ADP ↔ creatine + ATP). ATP phosphorylates glucose via hexokinase (ATP + glucose ↔ ADP + G-6-P). G-6-P then reduces the NAD^+ to NADH via G6-PDH (G-6-P + NAD^+ ↔ gluconate-6-P + NADH). The NAD^+ formed is stoichiometric with CK enzymatic kinetics at 340 nm.

2.5.3. Quantitative Assessment of Cellular Ion Dynamics

We measured the contents of Na^+, K^+, Ca^{2+}, Mg^{2+}, and Cl^- in the cardiac homogenate using tried-and-true methods described in the Teco, Randox, or Biosystems kits directory [27].

A pale-yellow precipitate is formed when sodium is mixed with magnesium uranyl acetate (Na + MgUrAc → NaMgUrAc). Ferrocyanide is added after solubilizing the precipitate with an ethanol/water combination. The resultant derivative takes on an intense orange hue proportional to sodium concentrations at 550 nm

Potassium ions and sodium tetraphenyl boron form a colloidal solution: K^+ + $(C_6H_5)_4BNa$ → $(C_6H_5)_4BK$ + Na^+. Solution turbidity is proportionate to potassium at 500 nm

In an alkaline environment (pH 10.7), calcium and O-Cresolphthalein complexone produce a violet chromogenic complex (Ca^{2+} + o-CPC → Ca^{2+}-CPC complex), with intensity commensurate with calcium contents at 578 nm.

Magonsulfonate, a metallochromic indicator, reacts with magnesium at pH 11.5 to produce a purple chromophore (Mg^{2+} + magonsulfonate → Mg^{2+}-magonsulfonate complex). This complex's intensity is instantly related to its magnesium content at 520 nm.

Chloride ions react with non-ionized mercuric thiocyanate, displace thiocyanate, and form an un-ionized mercury (II) chloride: $Hg(SCN)_2$ + $2Cl^-$ → HgCI2 + $2SCN^-$. The released thiocyanate ions react with ferric ions to produce a red complex [$3SCN^-$ + 4Fe3+ → $4Fe(SCN)_3$], whose luminance is proportional to the initial chloride contents at 480 nm.

Na/K-ATPase and Ca/Mg-ATPase degrade ATP to ADP and Pi (ATP + H_2O → ADP + Pi). Released Pi and malachite green dye produce a stable

complex (Pi + dye → Pi-dye complex), whose optical density relates with ATPase enzymatic activity at 660 nm [29].

2.5.4. Lipid parameters assessment

As specified in the LABKIT manual, cardiac triacylglycerol, cholesterol, and phospholipids contents were assessed [27].

Lipoprotein lipase breaks down triacylglycerol (TAG) into glycerol (G) and fatty acids (FAs): TAG + 3 H_2O → G + FAs. Glycerol kinase phosphorylates glycerol to form glycerol-3-phosphate (G3P): G + ATP → G3P + ADP. G3P dehydrogenase converts G3P into DHAP and H_2O_2, resulting in a red quinone imine dye with 4-amino antipyrine, 4-chlorophenol, and peroxidase (H_2O_2 + 4-AAP + 4-CPh → QI + HCl + 4 H_2O). Dye intensity at 546 nm specifies TAG content.

Cholesterol esterase transforms cholesterol ester into cholesterol (chol) and free fatty acids (chol-ester + H_2O → chol + FAs). Free cholesterol is oxidized by cholesterol oxidase to cholest-4-en-3-one and H_2O_2 (chol + O_2 → cholest-4-en-3-one H_2O_2). Quinone imine, a red chromogenic molecule is produced from phenol and 4-amino antipyrine (4-AAP) by hydrogen peroxide in the presence of peroxidase (H_2O_2 + Ph + 4-AAP → QI + 4 H_2O). At 500 nm, dye optical density and cholesterol levels are analogous.

Phospholipids (PLs) are converted to phosphatidic acids (PAs) and choline by phospholipase D (PLs + H_2O → PAs + choline). Choline is converted to betaine and hydrogen peroxide by choline oxidase (choline + 2 O_2 + H_2O → betaine + 2 H_2O_2). Red quinone imine (QI) dye is produced when H_2O_2 combines with dichlorophenol (DCPh) and 4-aminophenazone (4-AP) via peroxidase (H_2O_2 + 4-AP + DCPh → QI + 4 H_2O). The QI absorbance at 505 nm is proportional to the PLs content. The cholesterol-to-phospholipid ratio was calculated by dividing cholesterol by phospholipid.

2.5.5. Oxidative stress estimation

2.5.5.1. Reactive oxygen species (H_2O_2 and NO) estimation. Iodine is released from potassium iodide when hydrogen peroxide oxidizes it in an acidic environment (H_2O_2 + 2 H+ + 2 KI → 2 H_2O + 2 K^+ + I_2). The iodine subsequently combines with excess KI to form a deep yellow chromogenic molecule (I_2 + KI ↔ KI_3). At 390 nm the molecule intensity is directly correlated with H_2O_2 levels [30].

Arginine is converted to citrulline and nitric oxide by nitric oxide synthase [2 L-arginine + 6 O_2 + 3NADPH + 3 H^+ → 2 L-citrulline + 6NO + 6$NADP^+$ + 9 H_2O]. Oxygen converts NO to NO_2^- and NO_3^-. The NADPH-dependent nitrate reductase converts NO_3^- to NO_2^-. Eventually, NO_2^- with Griess reagents produce a red-violet chromophoric azo compound [NO_2^- + sulfanilamide/sulfanilic acid → diazonium salt, + N-(1-naphthyl)ethylenediamine → azo dye]. The chromogen dye intensity directly correlates to NO at 520 nm [31].

2.5.5.2. Antioxidant (GSH, GST, SOD, CAT, GPx) estimation. Standard chemical procedures were employed to assess reduced glutathione (GSH), glutathione-S-transferase (GST), superoxide dismutase (SOD), catalase (CAT), and glutathione peroxidase (GPx).

Reduced glutathione interacts with 5,5'-dithiobis(2-nitrobenzoic acid) (DTNB) to form oxidized glutathione and 2-nitro-5-thiobenzoic acid (TNB), a yellow chromogen [2GSH + DTNB → GSSG + TNB]. The increased TNB optical density at 420 nm corresponds to the GSH level [32].

Glutathione-S-transferase (GST) turns GSH and 1-chloro-2,4-dinitrobenzene (CDNB) into glutathione conjugate, a yellow chromophore (CDNB + GSH → CDNB-SG conjugate + HCl). The increased chromophore intensity at 340 nm relates to the CDNB-SG conjugate and, therefore, the GST enzyme activity [33].

Pyrogallol is transformed by superoxide anion radical to purpurogallin, a brown chromogenic molecule [pyrogallol + O_2^{*-} → purpurogallin], increasing the luminosity. SOD counteracts the superoxide anion (2 O_2^{*-}→ H_2O_2 + O_2), so inhibiting pyrogallol autoxidation. The decreased brown intensity is unswervingly related to the extent of pyrogallol autoxidation inhibition and SOD enzymatic activity at 420 nm [34].

Catalase decomposes hydrogen peroxide to water and oxygen (2 H_2O_2 → 2 H_2O + O_2). The unused H_2O_2 combines with ammonium molybdate to induce a yellow chromophoric complex (H_2O_2 + ammonium molybdate → molybdenum complex). At 405 nm, the complex-triggered drop in intensity is inversely related to the amount of unused H_2O_2 but directly related to catalase reactivity [35].

Glutathione peroxidase (GPx) breaks down hydrogen (organic) peroxide via GSH as a substrate to form alcohol and GSSG (H_2O_2 + 2GSH → 2 H_2O + GSSG). The leftover GSH reacts with DTNB to produce oxidized glutathione and 2-nitro-5-thiobenzoic acid (TNB), a yellow chromogenic substance [2GSH + DTNB → GSSG + TNB]. At 420 nm, the chromogen-evoked decline in intensity is directly proportionate to unreacted GSH but inversely proportionate to GPx kinetics [36].

2.5.5.3. Lipid peroxidation Marker (MDA) estimation. MDA, a representative of a thiobarbituric acid reactive substance (TBARS) and lipid peroxidation derivative, counteracts thiobarbituric acid (TBA) to evoke a pinked-color chromogenic product MDA + 2TBA → MDA-TBA complex). The chromogenic-elicited amplification in absorbance is uniformly related to the MDA quantity and the degree of lipid oxidative impairment at 523 nm [37].

2.5.6. Statistical analysis

Quantitative variables were expressed using the mean ± S.E.M. (n = 6 per group). Significant group differences were determined using one-way ANOVA and the Duncan Multiple Range Test, with $p<0.05$. All analyses utilized SPSS 20.0. GraphPad Prism 8.0 was employed to create all the graphs.

3. Results

3.1. Hesperidin reverses DDVP-elicited changes in protein and creatine kinase activity

The consequences of DDVP (8 $mg.kg^{-1}day^{-1}$), DDVP mixed with hesperidin (50 and 100 $mg.kg^{-1}day^{-1}$), or reference prescription atropine (0.2 $mg.kg^{-1}day^{-1}$) and hesperidin unaccompanied (50 and 100 $mg.kg^{-1}day^{-1}$) on total protein and creatine kinase isoenzyme myocardium (CK-MB) activity is exemplified in Fig. 1. Our study revealed that DDVP intoxication significantly ($p<0.05$) reduced heart total protein levels (14.74 %, Fig. 1a) and heart CK-MB activity (29.75 %, Fig. 1c) compared to the control group. Conversely, plasma CK-MB activity was significantly raised (176.79 %, Fig. 1b) by DDVP treatment. Regardless, hesperidin (at the stated doses) and atropine administration to DDVP-treated rats significantly reversed these dynamics, normalizing heart total protein levels and bringing plasma and heart CK-MB activity towards normal values. Interestingly, hesperidin supplementation in healthy rats did not affect heart or plasma protein levels or CK-MB activity compared to the healthy control group.

3.2. Hesperidin restores heart enzyme activity suppressed by DDVP exposure, with partial mitigation by atropine

Fig. 2 illustrates that DDVP (8 $mg.kg^{-1}day^{-1}$) spurred a significant ($p<0.05$) reduction in the activities of heart enzymes: AST (Fig. 2A) by 42.86 %, ALT (Fig. 2B) by 34.00 %, ALP (Fig. 2C) by 35.78 %, and LDH (Fig. 2D) by 15.92 %. On the other hand, post-administration of hesperidin (50- and 100 $mg.kg^{-1}day^{-1}$) restored the DDVP-initiated diminution in AST, ALP, and LDH activity to normal levels. Post-atropine administration, however, only partially restored these enzyme activities by mitigating the DDVP-induced reductions in heart enzyme activities

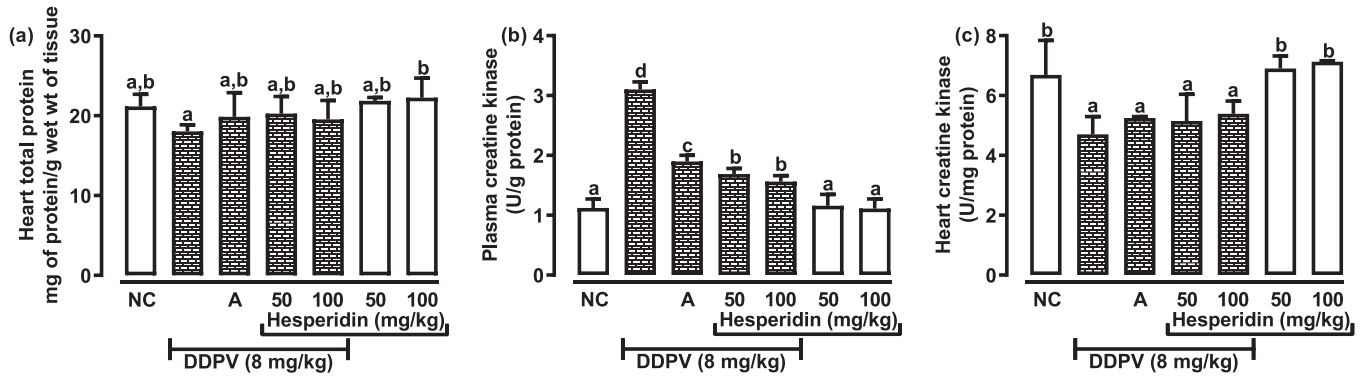

Fig. 1. The efficacy of Hes-7-RGlc 14 days subacute chemotherapeutic on DDVP-triggered changes in the total heart protein concentration (graph a), plasma creatine kinase activity (graph b), heart creatine kinase activity (graph c). NC signifies normal control, letter 'A' signifies atropine, while DDPV signifies dichlorvos or 2,2-dichlorovinyl dimethyl phosphate. The data are displayed as mean ± SEM (n = 6 rats/group). Significant ($P<0.05$) variations exist between bars denoted by varied typescripts.

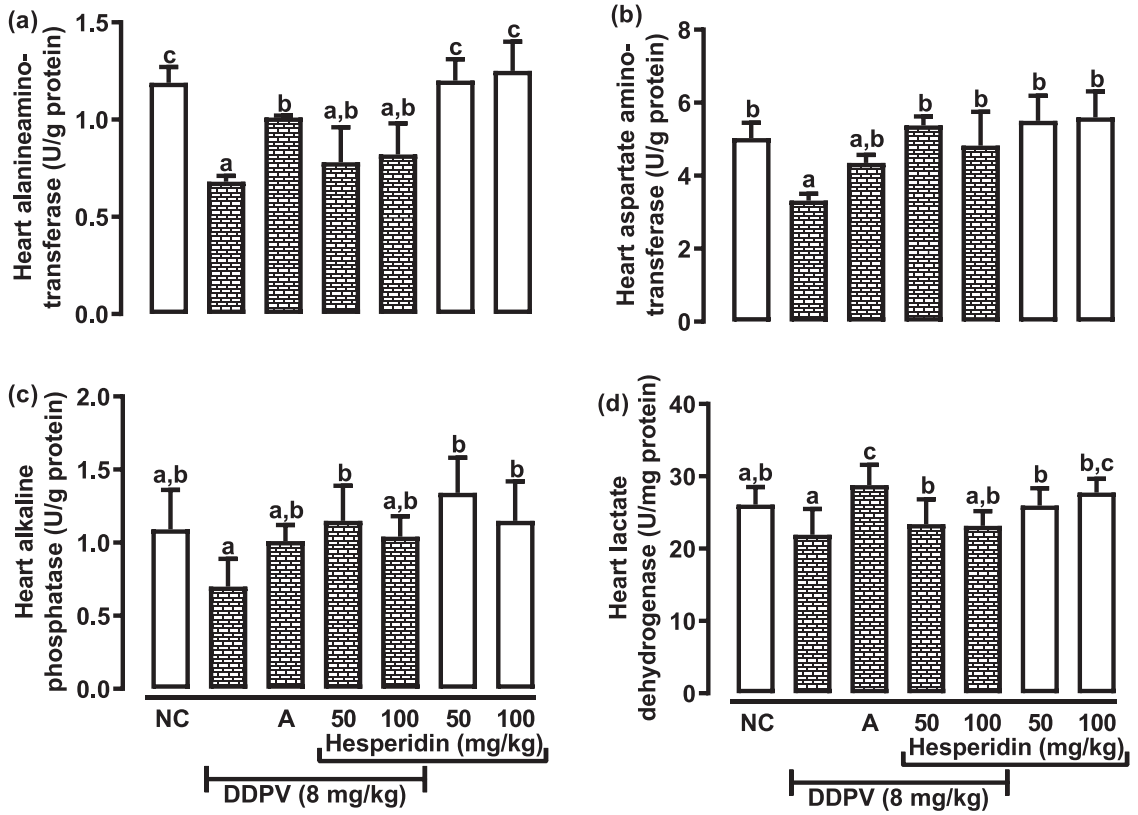

Fig. 2. The efficacy of Hes-7-RGlc 14 days subacute chemotherapeutic on DDVP-triggered heart changes in the activities of ALT (graph a), AST (graph b), ALP (graph c), and LDH (graph d). NC signifies normal control, letter 'A' signifies atropine, while DDPV signifies dichlorvos or 2,2-dichlorovinyl dimethyl phosphate. The data are displayed as mean ± SEM (n = 6 rats/group). Significant ($P<0.05$) variations exist between bars denoted by varied typescripts.

by 48.53 % for AST, 31.02 % for ALT, 44.29 % for ALP, and 31.14 % for LDH. Furthermore, hesperidin treatment in unexposed rats did not cause significant changes in enzyme activity levels compared to unexposed rats.

3.3. Hesperidin counteracts DDVP-provoked alterations in cardiac electrolyte levels

The outcome of DDVP ($mg.kg^{-1}day^{-1}$) and hesperidin (50 and 100 $mg.kg^{-1}day^{-1}$) on heart electrolyte levels is demonstrated in Fig. 3. DDVP significantly alters cardiac electrolyte contents. Specifically, DDVP elicited a decrease in magnesium (Mg) by 30.84 % ($p<0.05$) while paradoxically increasing sodium (Na) and calcium (Ca) levels by 34.23 % and 46.34 %, respectively ($p<0.05$). Fascinatingly, potassium (K) levels remained unchanged. Nonetheless, hesperidin administration significantly ($p<0.05$) countered the DDVP-precipitated alterations in cardiac electrolyte concentrations. It reinstated Mg and Ca to normal levels and brought Na levels close to normal, with adjustments of 42.47 %, 7.94 %, and 11.41 %, respectively. In addition, healthy rats treated with hesperidin did not cause significant ($p>0.05$) changes in cardiac electrolyte levels compared to the control group.

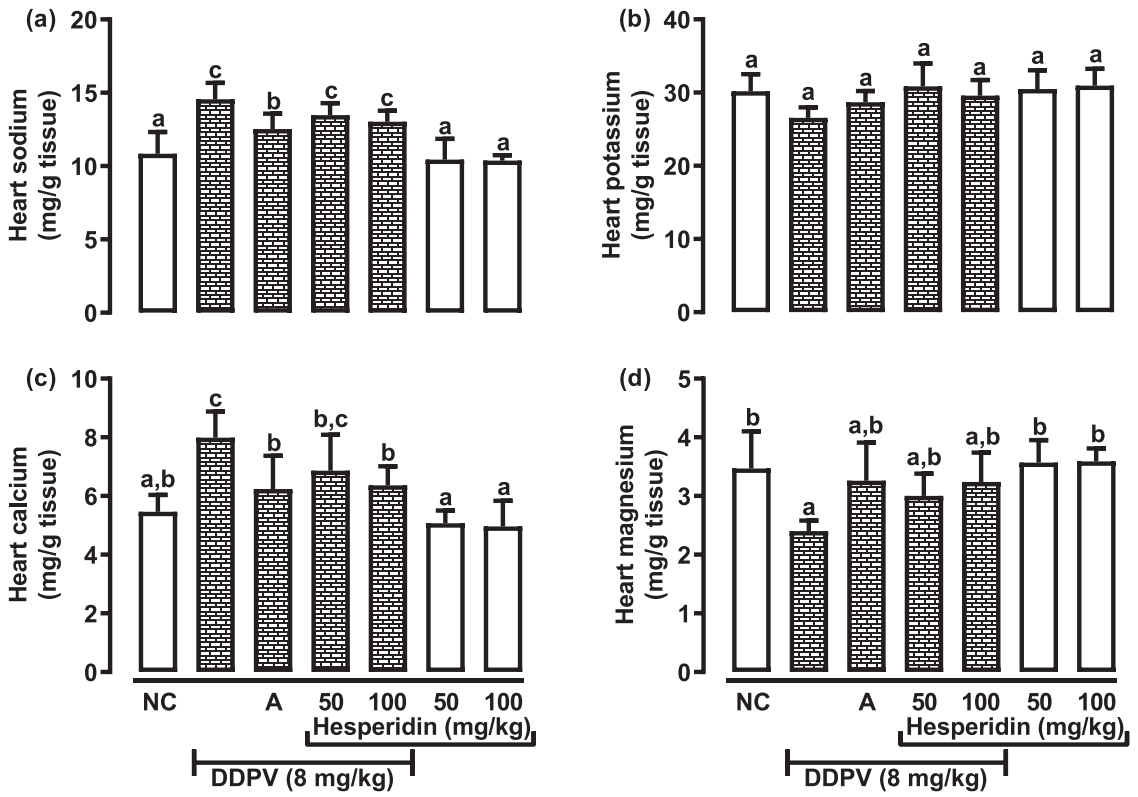

Fig. 3. The efficacy of Hes-7-RGlc 14 days subacute chemotherapeutic on DDVP-triggered heart changes in the concentrations of sodium (graph a), potassium (graph b), calcium (graph c), and magnesium (graph d). NC signifies normal control, letter 'A' signifies atropine, while DDPV signifies dichlorvos or 2,2-dichlorovinyl dimethyl phosphate. The data are displayed as mean ± SEM (n = 6 rats/group). Significant ($P<0.05$) variations exist between bars denoted by varied typescripts.

3.4. Mitigatory efficacy of hesperidin and atropine on DDVP-mediated cardiac ion pump dysfunction

Post hesperidin supplementation (50 and 100 mg.kg^{-1}day^{-1}) or post-atropine (at 0.2 mg.kg^{-1}day^{-1}) intervention on DDVP-induced alterations on the heart chloride level and Na/K and Ca/Mg ATPase activities is highlighted in Fig. 4. DDVP significantly ($p<0.05$) abated the Na/K-ATPase (Fig. 4a) and Ca/Mg ATPase (Fig. 4b) activities by 30.94 % and 38.13 %, respectively. Captivatingly, DDVP did not cause any significant changes in heart chloride contents (Fig. 4a). On the contrary, supplementation with either hesperidin (at doses of 50 and 100 mg/kg body weight per day) or atropine (0.2 mg/kg body weight per day) after DDVP exposure significantly ameliorated these detrimental consequences and restored the activity of both ion pumps to normal levels. Outstandingly, hesperidin administration in healthy rats did not alter cardiac electrolyte levels compared to the control group.

3.5. Hesperidin ameliorates DDVP-triggered disruptions in heart and plasma dyslipidemia in rats

Fig. 5 illustrates the effects of hesperidin supplementation (50 and 100 mg.kg^{-1}day^{-1}), as well as the reference compound atropine (0.2 mg/kg/day), on DDVP-engendered changes in heart and plasma lipid profiles. Significant alterations ($p<0.05$) were observed in the lipid profiles of the DDVP-treated group. Specifically, there were remarkable increases in plasma cholesterol (77.57 %, Fig. 5b), plasma phospholipids (43.39 %, Fig. 5c), plasma cholesterol/phospholipid ratio (23.89 %, Fig. 5d), LDL cholesterol (124.11 %, Fig. 5g), heart cholesterol

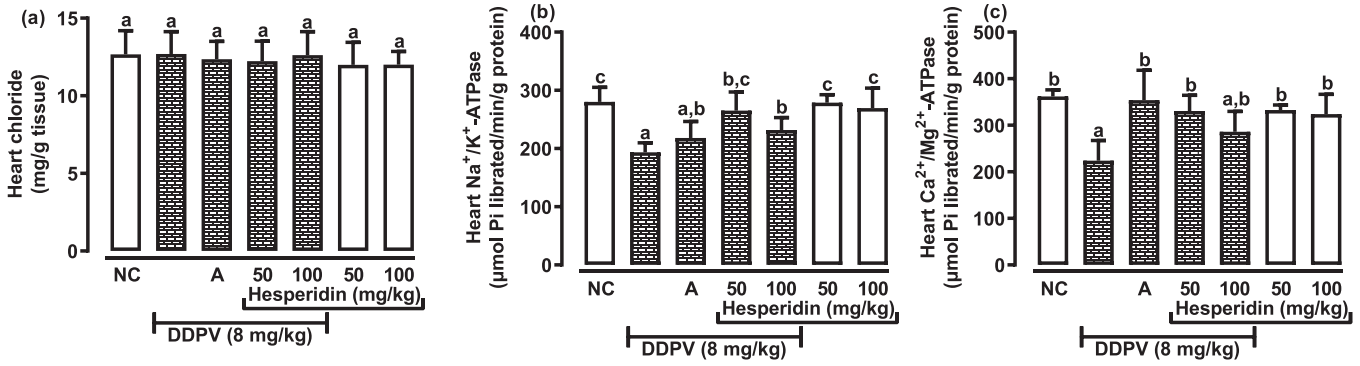

Fig. 4. The efficacy of Hes-7-RGlc 14 days subacute chemotherapeutic on DDVP-triggered heart changes in the chloride concentration (graph a), Na^+/K^+-ATPase activity (graph b), and Ca^{2+}/Mg^{2+}-ATPase activity (graph c). NC signifies normal control, letter 'A' signifies atropine, while DDPV signifies dichlorvos or 2,2-dichlorovinyl dimethyl phosphate. The data are displayed as mean ± SEM (n = 6 rats/group). Significant ($P<0.05$) variations exist between bars denoted by varied typescripts.

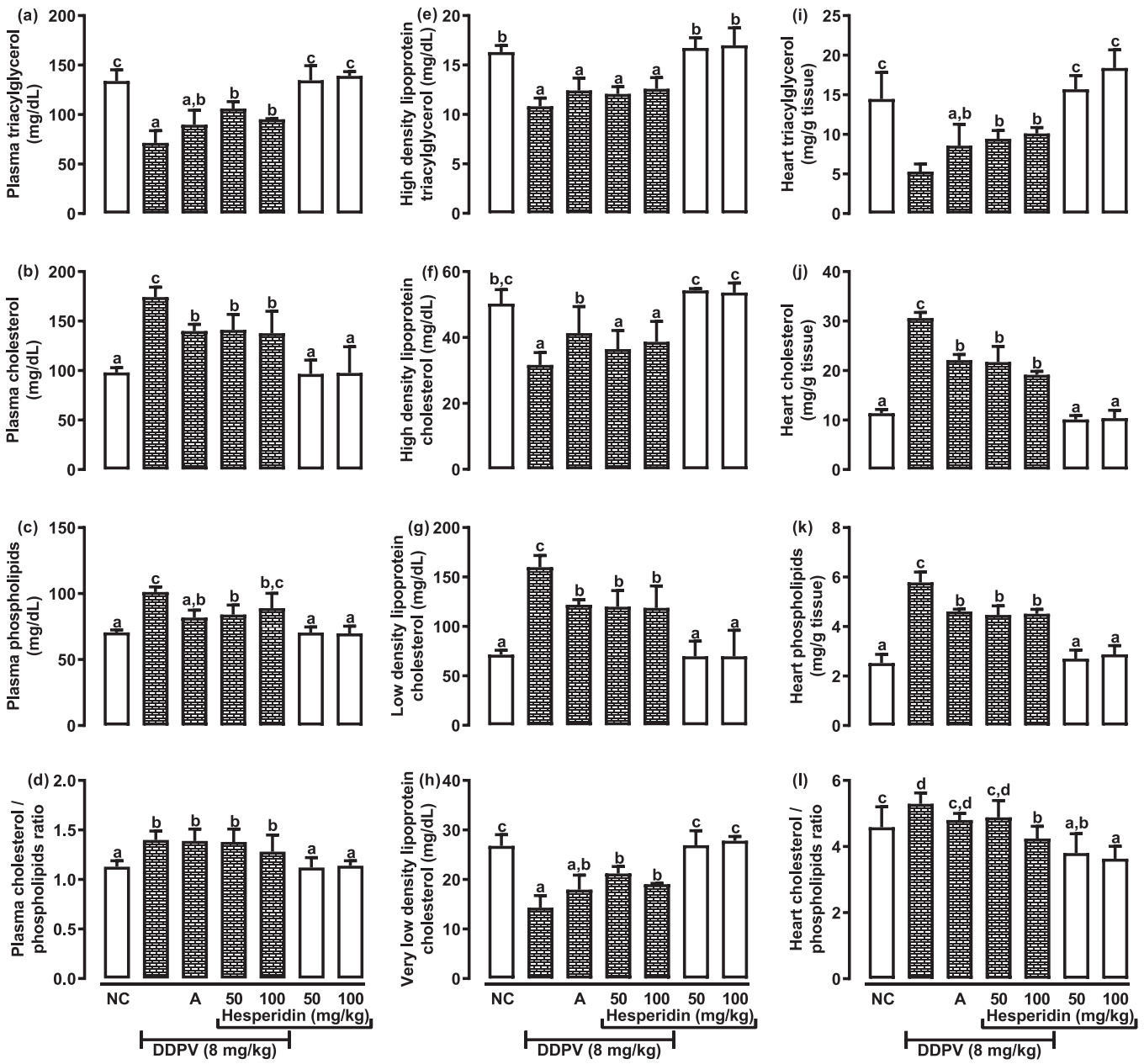

Fig. 5. The efficacy of Hes-7-RGlc 14 days subacute chemotherapeutic on DDVP-triggered changes in the concentrations of plasma triacylglycerol (graph a), plasma cholesterol (graph b), plasma phospholipids (graph c), plasma cholesterol/phospholipids rations (graph d), HDL triacylglycerol (graph e), HDL cholesterol (graph f), LDL cholesterol (graph g), VLDL cholesterol (graph h), heart triacylglycerol (graph i), heart cholesterol (graph j), heart phospholipids (graph k), and heart cholesterol/phospholipids rations (graph l). NC signifies normal control, letter 'A' signifies atropine, while DDPV signifies dichlorvos or 2,2-dichlorovinyl dimethyl phosphate. The data are displayed as mean ± SEM (n = 6 rats/group). Significant ($P<0.05$) variations exist between bars denoted by varied typescripts.

(169.07 %, Fig. 5j), heart phospholipids (129.37 %, Fig. 5k), and heart cholesterol/phospholipid ratio (15.50 %, Fig. 5l). Conversely, significant decreases ($p<0.05$) were observed in plasma TAG (46.59 %, Fig. 5a), HDL TAG (33.60 %, Fig. 5e), HDL cholesterol (37.06 %, Fig. 5f), VLDL cholesterol (46.58 %, Fig. 5h), and heart TAG (63.37 %, Fig. 5i) when compared to the normal control group.

Two weeks of post-intervention with either hesperidin (50 and 100 mg/kg) or atropine in DDVP-treated rats significantly ($p<0.05$) attenuated these lipid profile disruptions to varying degrees. Additionally, hesperidin administration in healthy rats did not induce any statistically significant ($p>0.05$) changes in their heart and plasma lipid profiles compared to the control group.

3.6. Protective effects of atropine and hesperidin on DDVP-stimulated H_2O_2 and NO accumulations in plasma and heart

The impact of DDVP (8 $mg.kg^{-1}day^{-1}$), atropine (0.2 $mg.kg^{-1}day^{-1}$)), and hesperidin (50- and 100 $mg.kg^{-1}day^{-1}$) intake on H_2O_2 and NO concentrations in both plasma and the heart. The data reveal significant increases ($p<0.05$) in heart and plasma H_2O_2 and NO concentrations in DDVP-treated rats compared to controls, with increases of 1.82-fold and 1.68-fold for heart and plasma H_2O_2, and 21.86-fold and 3.02-fold for heart and plasma NO, respectively.

However, co-administration of atropine and hesperidin significantly ($p<0.05$) mitigated these increases. Specifically, in the heart, H_2O_2 levels were reduced by 34.39 %, 26.09 %, and 32.81 %, and NO contents by 21.09 %, 15.27 %, and 21.45 % following treatment with

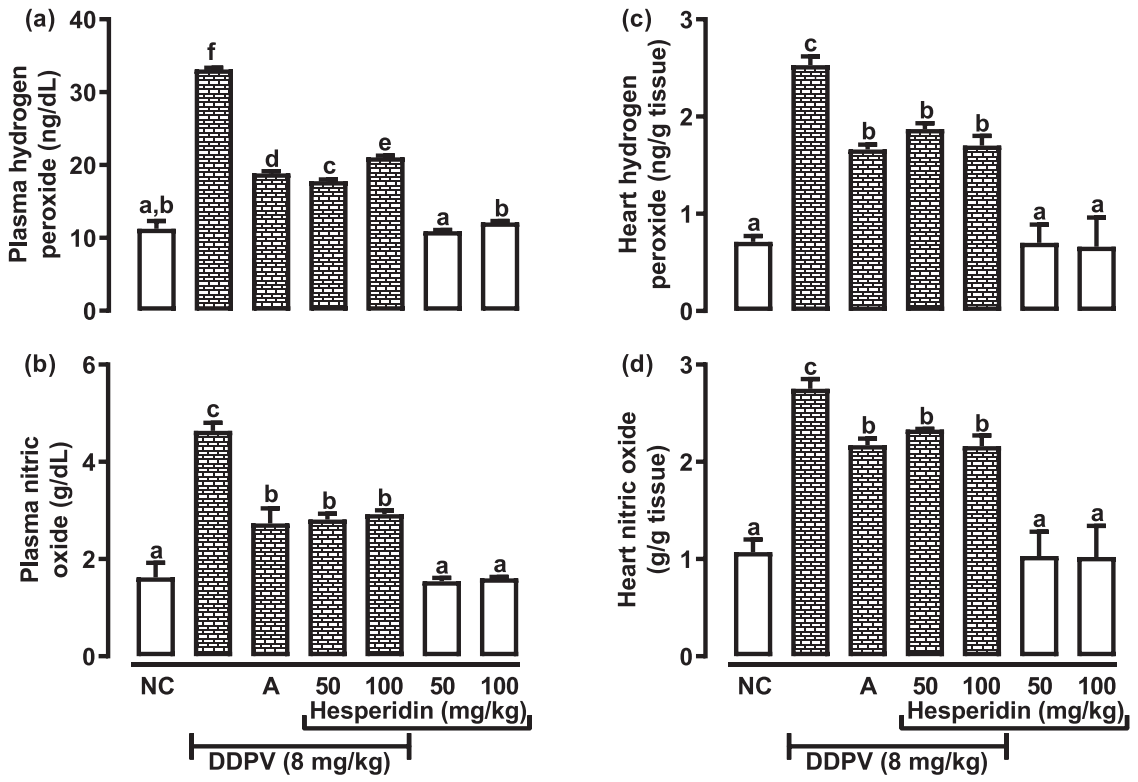

Fig. 6. The efficacy of Hes-7-RGlc 14 days subacute chemotherapeutic on DDVP-triggered changes in the concentrations of plasma H_2O_2 (graph a), plasma NO (graph b), heart H_2O_2 (graph c), and heart NO (graph d). NC signifies normal control, letter 'A' signifies atropine, while DDPV signifies dichlorvos or 2,2-dichlorovinyl dimethyl phosphate. The data are displayed as mean ± SEM (n = 6 rats/group). Significant ($P<0.05$) variations exist between bars denoted by varied typescripts.

atropine and hesperidin. In the plasma, H2O2 levels decreased by 43.08 %, 46.31 %, and 36.40 %, while NO levels were reduced by 41.16 %, 39.44 %, and 37.07 %.

Prominently, treatment of normal rats with hesperidin did not result in significant differences ($p>0.05$) in heart or plasma H2O2 or NO levels compared to the control group.

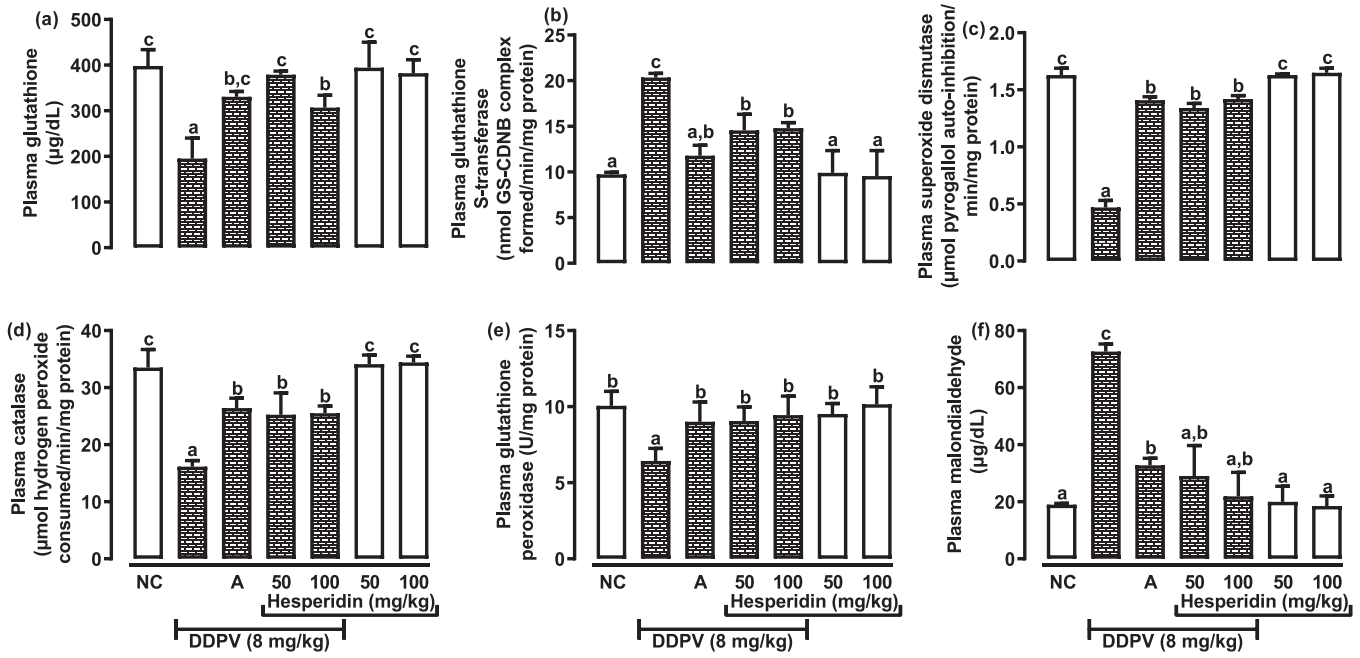

Fig. 7. The efficacy of Hes-7-RGlc 14 days subacute chemotherapeutic on DDVP-triggered plasms changes in the concentrations of GSH (graph a) and MDA (graph f) as well as the activities of GST (graph b), SOD (graph c), catalase (graph d) and GPx (graph e). NC signifies normal control, letter 'A' signifies atropine, while DDPV signifies dichlorvos or 2,2-dichlorovinyl dimethyl phosphate. The data are displayed as mean ± SEM (n = 6 rats/group). Significant ($P<0.05$) variations exist between bars denoted by varied typescripts.

3.7. Hesperidin and atropine ameliorate DDVP-initiated plasma oxidative stress

Fig. 7 showcases the effectiveness of hesperidin supplementation (50 and 100 mg.kg^{-1}day^{-1}) and reference atropine (0.2 mg.kg^{-1}day^{-1}) in mitigating DDVP-triggered alterations in plasma antioxidant status. DDVP exposure in rats elicited significant reductions ($p<0.05$) in plasma GSH levels and the activities of antioxidant enzymes SOD, catalase, and GPx by 51.00 %, 71.17 %, 51.76 %, and 36.02 %, respectively. Contrariwise, GST activity and MDA level, a biomarker of oxidative stress, were significantly ($p<0.05$) elevated by 109.15 % and 186.42 %, respectively, compared to the control group.

Pleasingly, post-treatment with either atropine or hesperidin (at both 50 and 100 mg/kg/day) for two weeks in DDVP-treated rats significantly ($p<0.05$) attenuated these DDVP-stimulated dynamics in plasma antioxidant markers. Atropine improved GSH, GST, SOD, CAT, GPx, and MDA levels by 69.61 %, 42.06 %, 200.00 %, 63.49 %, 39.97 %, and 54.84 %, respectively. Hesperidin supplementation (50 mg/kg/day) exhibited similar protective effects, increasing GSH, GST, SOD, CAT, and GPx, and decreasing MDA levels by 94.26 %, 28.50 %, 185.11 %, 56.31 %, 40.75 %, and 60.00 %, respectively. Conspicuously, hesperidin at 100 mg/kg/day provided comparable benefits, improving GSH, GST, SOD, CAT, and GPx, and reducing MDA levels by 57.28 %, 27.27 %, 202.13 %, 57.80 %, 46.97 %, and 69.86 %, respectively.

Outstandingly, hesperidin administration in healthy rats did not cause significant ($p>0.05$) changes in their plasma antioxidant status compared to the control group.

3.8. Impact of DDVP and hesperidin on cardiac antioxidant biomarkers: protective effects and comparative analysis

The effects of DDVP (8 mg.kg^{-1}day^{-1}), hesperidin supplementation (50 and 100 mg.kg^{-1}day^{-1}) combined with DDVP, reference atropine (0.2 mg.kg^{-1}day^{-1}), and hesperidin alone (50 and 100 mg/kg/day) on cardiac antioxidant biomarkers. DDVP exposure significantly ($p<0.05$) altered antioxidant markers in the heart. DDVP significantly ($p<0.05$) decreased cardiac levels of GSH (17.97 %, Fig. 8a), GST activity (56.87 %, Fig. 8b), SOD activity (39.27 %, Fig. 8c), and GPx activity (52.31 %, Fig. 8e). Conversely, DDVP significantly increased ($p<0.05$) CAT activity (42.53 %, Fig. 8d) and MDA levels (195.24 %, Fig. 8f), indicating oxidative stress. Post-treatment with either atropine or hesperidin (both doses) for two weeks significantly ($p<0.05$) reversed these DDVP-induced alterations in cardiac antioxidant status. GSH, CAT, and GPx activities were restored to normal levels. GST, SOD, and MDA levels were also significantly reduced by atropine and hesperidin (at both doses) compared to the DDVP group. Notably, hesperidin administration in healthy rats did not cause significant changes ($p>0.05$) in cardiac antioxidant markers compared to the control group.

4. Discussion

The presence of pesticides, such as dichlorvos (DVDP), in edible agricultural products [5] is a significant threat to human health, leading to excruciating ailment and death, especially in third-world nations [2, 3]. Hesperetin-7-O-rhamnoglucoside (Hes-7-RGlc) has been enlisted to reverse xenobiotic detrimental impacts [18]. This inquiry looked into the therapeutic impact of Hes-7-RGlc on ameliorating DVDP-facilitated cardiotoxicity in rats. The result depicts that Hes-7-RGlc efficiently abolished the DDVP, which triggered negative cardiac consequences.

This current probe showed that DDVP toxicosis markedly raised plasma creatine kinase (CK) activity, portending cardiac muscle damage or boosting muscle membrane permeability [38]. DDVP also noticeably declined heart total protein and heart CK-MB action, connoting accelerated cardiac protein catabolism or diminished protein anabolism [39]. This alteration of CK-MB and protein in the two compartments could provoke cardiac muscle weakness, downsize structural probity, sabotage cardiac ATP bioenergetics and metabolism, rhabdomyolysis, and heart failure [38,39].

Nonetheless, we observed that Hes-7-RGlc annulled these DDVP-instigated altered biomarkers in rat plasma and heart by normalizing the CK-MB activity and protein content; this could be via Hes-7-RGlc cytomembrane preservation property [17].

While ALT transaminates L-alanine to pyruvate, AST transaminates L-aspartate to oxaloacetate. ALT is predominantly situated in the liver;

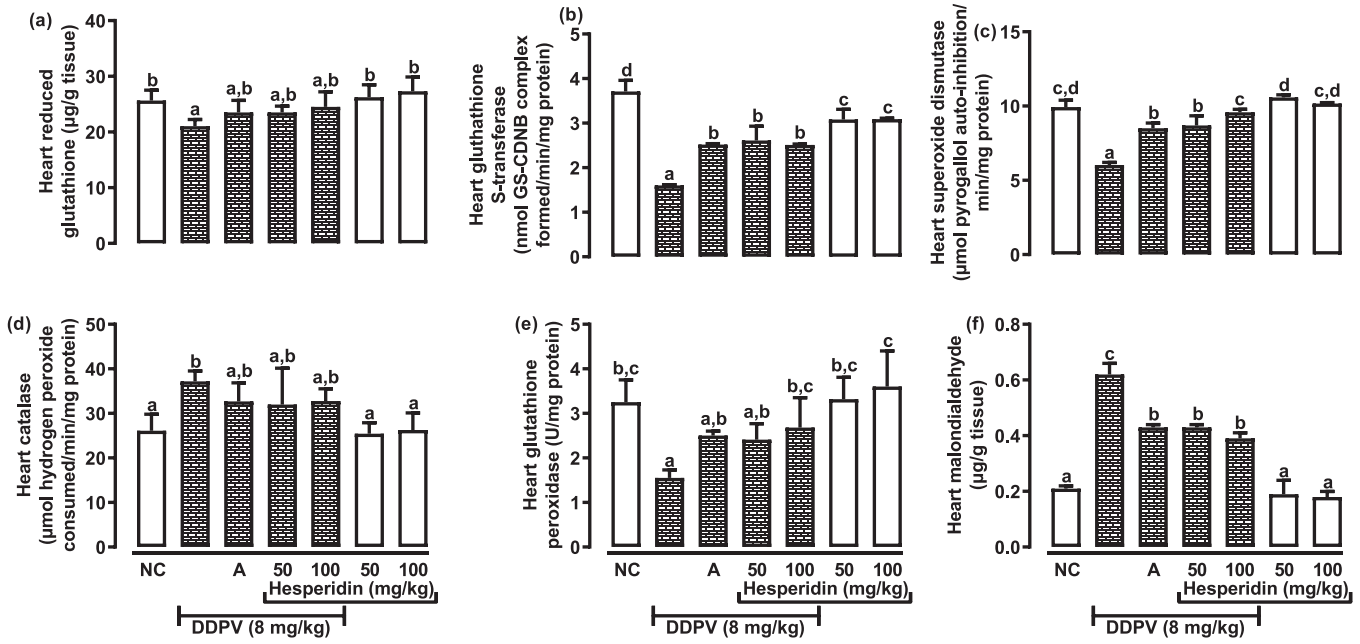

Fig. 8. The efficacy of Hes-7-RGlc 14 days subacute chemotherapeutic on DDVP-triggered heart changes in the concentrations of GSH (graph a) and MDA (graph f) as well as the activities of GST (graph b), SOD (graph c), catalase (graph d) and GPx (graph e). NC signifies normal control, letter 'A' signifies atropine, while DDPV signifies dichlorvos or 2,2-dichlorovinyl dimethyl phosphate. The data are displayed as mean ± SEM (n = 6 rats/group). Significant (P<0.05) variations exist between bars denoted by varied typescripts.

however, small quantities are present in the extra-hepatic compartment, including heart muscle. In that order, the heart contains the highest AST, followed by the liver, skeletal muscle, kidney, and brain, and has been used to predict cardiac crisis [40]. ALP dephosphorylates and degrades proteins. LDH reversibly reduces pyruvic acid to lactic acid with concomitant energy production, especially in a hypoxic state. Apart from skeletal muscle, the heart is the second organ with the highest LDH contents [41]. Elevated plasma LDH and ALP and depleted heart LDH and ALP have been implicated in cardiovascular dysfunction [42,43]. The current study found that DDVP strikingly decreased cardiac ALT, AST, ALP, and LDH, substantiating the documentation of Dwivedi et al. [44], signifying disruption of these enzyme structures and functions leading to metabolic dyshomeostasis. The recorded derangement might be ascribed to DDVP-prompted cellular leakage, enzyme inhibition, or escalated ROS generation owing to mitochondria dysfunction [45].

Rekindling these enzyme actions shows that Hes-7-RGlc post-administration could preserve cardiac enzymes and mitochondrial integrity, shape, and function. Its antioxidant and cytomembrane stabilizing properties may have mitigated cardiac damage and improved enzyme function [20].

This investigation observed that DDVP initiates heart hypomagnesemia, hypernatremia, and hypercalcemia while regressing Na/K-ATPase and Ca/Mg ATPase activities. Meanwhile, potassium and chloride were not altered. The electrolyte and ionic pump dysregulation could undermine various physiological systems and functions, resulting in myriad complications including neuromuscular issue such as contractility and arrhythmias [46]; cardiovascular condition such as hypertension and blood clotting [47], metabolic crises such as ATP, nucleic acid and protein synthesis inhibition [48], bone demineralization such as bone resorption and osteoporosis [49], psychological, neurological, and cellular depolarization disorders [46]. The underpinning mechanism by which Hes-7-RGlc supplementation restored this electrolyte dysregulation could be associated with its impact on ion channels and its antioxidant propensities [21].

In this research, DDVP evoked mixed dyslipidemia characterized by intensified cholesterol, phospholipids, and cholesterol/phospholipid ratio in the plasma and heart tissues. Elevated cholesterol was also noted in LDL and VLDL. In contrast, TAG contents in plasma, HDL, heart, and HDL-cholesterol notably plummeted.

These distorters suggest skyrocketed plasma hypercholesterolemia and hyperphospholipidemia as well as heightened cardiac cholesterogenesis and phospholipidosis, lowered membrane fluidity, lipid signaling processes, ATP biosynthesis, and reversed cholesterol transport [50]. These events would ultimately lead to atherosclerosis, cardiac dysfunction, arrhythmias, and heart failure [51]. DDVP has been earlier reported to perturb the lipid milieu [52]. The spotted mixed dyslipidemia could be caused by DDVD-spurred lipid metabolizing enzyme inhibition, oxidative stress, or inflammation [50–52].

Regardless, Hes-7-RGlc post-administration shows efficiency in taming, attenuating, and mitigating DDVD-incited lipid dysmetabolism, insinuating their capacity to reverse cardiotoxicity and regularize heart function might be credited to its aptitude to scavenge unstable free radicals, improving lipid metabolizing enzymes, bolster lipid clearance, and abate lipid oxidation [22].

In this exploration, we glimpsed that DDVP-occasioned amplified cardiac and plasma concentration of H_2O_2, NO, and malondialdehyde and diminished the GSH levels as well as the activities of GST, SOD, catalase, and glutathione peroxidase. Generally, OP compounds, including DDVP, exert neurotoxicity by inhibiting neuronal cholinesterase [11]. Studies have shown that DDVP also exerts cytotoxicity by aggravating reactive species and oxidative stress [14].

Endothelial cells and immune cells such as macrophages and neutrophils continuously release H_2O_2 to kill pathogens and NO, an endothelial-derived relaxing factor to promote vasodilation [53]. While H_2O_2 and NO are a critical signaling molecule involved in various physiological processes, excessive or dysregulated formation of H_2O_2 and NO in the heart, vascular vessel, or blood could lead to hypotension, oxidative stress, inflammation via activation of transcription factors such as nuclear factor-kappa B (NF-κB), tissue damage, and remodeling, contributing to the pathogenesis of cardiovascular diseases and heart dysfunction [54].

In addition, these cells produce electrons during normal cellular mitochondrial respiration. The leakage of electrons from the mitochondrial electron transport chain leads to the partial reduction of oxygen molecules to form superoxide radicals (O_2^{*-}). Subsequent dismutation of O_2^{*-} SOD engenders H_2O_2. The dappled receded SOD could be that DDVP invoked NADPH oxidase, an enzyme that catalysis the production of O_2^{*-}, which then overwhelmed the SOD. Catalase or GPx then degrade H_2O_2 to water. GPx uses GSH as a cofactor. The cardiac and plasma depletion in the antioxidant peptide/proteins, as well as accrued MDA, a marker of lipid peroxidation, could be due to excessive accumulation of free radicals, resulting in circulating oxidatively stressed plasma and cardiac dysfunction [55,56].

Captivatingly, Hes-7-RGlc efficaciously mitigated the DDVD-elicited ROS buildup and oxidative stress reversal, signals its ability to obliterate cardiotoxicity and reinstate heart function might be attributed to its ability to mop up ROS and augment/up-regulate antioxidative peptide/enzymes biosynthesis, and rescind lipid peroxidation [17,18,22].

Though atropine showed partial reinstatement of most of the assay parameters, hesperidin depicted superior efficacy in restoring these measured biomarkers, indicating that hesperidin may provide supplementary shielding aids outside the atropine cholinergic influence maybe by its multi-targeted antioxidative and anti-inflammatory mechanisms.

Although Hes-7-RGlc is seen in different fruits, mainly citrus fruits, its intake differs greatly subject to a person's dietary habits. On the other hand, the dosage of DVDP used in this study on rats compared to the minimum average human exposure is 1:125. Thus, Hes-7-RGlc can be backed as a promising natural adjunct or supplementary drug candidate and mitigator of DVDP-mediated intoxication via its capacity to normalize deranged electrolytes, ion pumps, redox status, lipid homeostasis.

Funding

No funding was received.

CRediT authorship contribution statement

Abiola F. Adenowo: Visualization, Supervision, Resources, Project administration. **Florence Anifowose:** Visualization, Supervision, Resources, Project administration. **Olufemi M. Ajagun-Ogunleye:** Visualization, Supervision, Resources, Project administration. **Adio J. Akamo:** Writing – review & editing, Writing – original draft, Visualization, Validation, Supervision, Resources, Project administration, Methodology, Funding acquisition, Conceptualization. **Ofem E. Eteng:** Visualization, Supervision, Resources, Project administration. **Adetutu O. Ojelabi:** Writing – original draft, Visualization, Validation, Resources, Methodology, Investigation, Funding acquisition, Formal analysis, Conceptualization. **Jacob K. Akintunde:** Visualization, Supervision, Resources, Project administration. **Oluwatobi Somade:** Writing – review & editing, Visualization, Resources, Project administration. **Iyabode A. Kehinde:** Visualization, Supervision, Resources, Project administration. **Regina N. Ugbaja:** Writing – review & editing, Visualization, Validation, Supervision, Project administration, Methodology, Conceptualization. **Adewale M. Taiwo:** Writing – review & editing, Visualization, Validation, Supervision, Project administration, Methodology, Conceptualization. **Boluwatife A. Olagunju:** Writing – original draft, Visualization, Validation, Resources, Methodology, Investigation, Funding acquisition, Formal analysis, Conceptualization. **Mushafau A. Akinsanya:** Visualization, Supervision, Resources, Project administration. **Adebisi A. Adebisi:** Visualization, Supervision, Resources, Project administration. **Tobi S. Adekunbi:** Visualization,

Supervision, Resources, Project administration.

Declaration of Competing Interest

The authors declare that they have no known competing financial interests or personal relationships that could have appeared to influence the work reported in this paper

Data availability

Data will be made available on request.

Acknowledgement

None.

References

[1] C.C. Ozoemena, F.U. Igwe, E.O. Nwachuku, E.S. Bartimaeus, Evaluation of 2, 2-dichlorovinyl dimethyl phosphate (sniper) induced hepatotoxicity and oxidative stress in New Zealand white rabbits, Int. Res. J. Gastroenterol. Hepatol. 4 (2) (2021) 52–65.
[2] H.U. Okoroiwu, I.A. Iwara, Dichlorvos toxicity: a public health perspective, Inter. Toxicol. 11 (2) (2018) 129.
[3] B.K. Binukumar, B. Amanjit, J.L. Ramesh, D.P. Kiran, Nigrostriatal neuronal death following chronic dichlorvos exposure: crosstalk between mitochondrial impairments, α synuclein aggregation, oxidative damage and behavioral changes, Mol. Brain. 3 (2010) 5.
[4] H.A. Abdel-Aziz, W. Mubarak, H.Z. Mohamed, M.W. Wadie, Effect of vitamin E supplementation on dichlorvos-induced toxicity in the hippocampus of male albino rat: a light-microscopic study, J. Curr. Med. Res. Pr. 7 (1) (2022) 69–73.
[5] A. Heshmati, F. Nazemi, Dichlorvos (DDVP) residue removal from tomato by washing with tap and ozone water, a commercial detergent solution and ultrasonic cleaner, Food Sci. Technol. 38 (2017) 441–446.
[6] W.J. Hayes, E.R. Laws, Handbook of Pesticide Toxicology, 3, Academic Press Inc, New York, 1990. Classes of Pesticides.
[7] Y. Zhang, W. Zhang, J. Li, S. Pang, S. Mishra, P. Bhatt, S. Chen, Emerging technologies for degradation of dichlorvos: a review, Int. J. Environ. Res. Pub. Health 18 (11) (2021) 5789.
[8] K.A. O'Leary, J.W. Tracy, Schistosoma mansoni: glutathione S-transferase-catalyzed detoxication of dichlorvos, Exp. Parasitol. 72 (4) (1991) 355–361.
[9] T. Katagi, T. Fujisawa, Acute toxicity and metabolism of pesticides in birds, J. Pest. Sci. 46 (4) (2021) 305–321.
[10] W. Boedeker, M. Watts, P. Clausing, E. Marquez, The global distribution of acute unintentional pesticide poisoning: estimations based on a systematic review, BMC Public Health 20 (2020) 1–19.
[11] M.R. Salahshoor, A. Abdolmaleki, A. Shabanizadeh, A. Jalali, S. Roshankhah, Ipomoea aquatica extract reduces hepatotoxicity by antioxidative properties following dichlorvos administration in rats, J. Physiol. Invest. 63 (2) (2020) 77–84.
[12] Y. Hou, Y. Zeng, S. Li, L. Qi, W. Xu, H. Wang, C. Sun, Effect of quercetin against dichlorvos induced nephrotoxicity in rats, Exp. Toxicol. Pathol. 66 (4) (2014) 211–218.
[13] I. Celik, Z. Yilmaz, V. Turkoglu, Hematotoxic and hepatotoxic effects of dichlorvos at sublethal dosages in rats, Environ. Toxicol.: Inter. J. 24 (2) (2009) 128–132.
[14] Y. El-Nahhal, I. El-Nahhal, Cardiotoxicity among children accidentally exposed to organophosphate insecticides coupled with scorpion bites in Gaza, Health 13 (9) (2021) 1045–1063.
[15] A. Imam, N.A. Sulaiman, A.L. Oyewole, S. Chengetanai, V. Williams, M.I. Ajibola, M.S. Ajao, Chlorpyrifos-and dichlorvos-induced oxidative and neurogenic damage elicits neuro-cognitive deficits and increases anxiety-like behavior in wild-type rats, Toxics 6 (4) (2018) 71.
[16] R. Hou, H. Zhang, H. Chen, Y. Zhou, Y. Long, D. Liu, Total pancreatic necrosis after organophosphate intoxication, Front. Med. 13 (2019), 285–258.
[17] S. Hosawi, Current update on role of hesperidin in inflammatory lung diseases: chemistry, pharmacology, and drug delivery approaches, Life 13 (4) (2023) 937.
[18] O.A.A. Mostafa, F. Ibrahim, E. Borai, Protective effects of hesperidin in cyclophosphamide-induced parotid toxicity in rats, Sci. Rep. 13 (1) (2023) 158.
[19] M. Vabeiryureilai, K. Lalrinzuali, G. Jagetia, Determination of anti-inflammatory and analgesic activities of a citrus bioflavanoid, hesperidin in mice, Immunochem. Immunopathol. 1 (107) (2015) 2.
[20] Y.A. Ali, O.M. Ahmed, H.A. Soliman, M. Abdel-Gabbar, M. Al-Dossari, N.S. Abd El-Gawaad, E. El-Nahass, N.A. Ahmed, Rutin and hesperidin alleviate paclitaxel-induced nephrocardiotoxicity in Wistar rats via suppressing the oxidative stress and enhancing the antioxidant defense mechanisms, Evid. Based Complement. Altern. Med. 2023 (2023) 5068304.
[21] Q. Xie, S. Gao, M. Lei, Z. Li, Hesperidin suppresses ERS-induced inflammation in the pathogenesis of non-alcoholic fatty liver disease, Aging (Albany NY) 14 (3) (2022) 1265.
[22] K. Kawabata, Y. Yoshioka, J. Terao, Role of intestinal microbiota in the bioavailability and physiological functions of dietary polyphenols, Molecules 24 (2) (2019) 370.
[23] N. Percie du Sert, V. Hurst, A. Ahluwalia, S. Alam, M.T. Avey, M. Baker, H. Würbel, The ARRIVE guidelines 2.0: updated guidelines for reporting animal research, J. Cereb. Blood Flow. Metab. 40 (9) (2020) 1769–1777.
[24] C.A. Görmeli, K. Saraç, O. Çiftçi, N. Timurkaan, S. Malkoç, The effects of Hes-7-RGlc on idiopathic pulmonary fibrosis evaluated by histopathologial-biochemical and micro-computed tomography examinations in a bleomycin-rat model, Biomed.. Res. 27 (2016) 737–742.
[25] A.O. Abolaji, M.U. Omozokpia, O.J. Oluwamuyide, T.E. Akintola, E.O. Farombi, Rescue role of Hes-7-RGlc in 4-vinylcyclohexene diepoxide-induced toxicity in the brain, ovary and uterus of wistar rats, J. Basic Clin. Physiol. Pharmacol. 31 (2) (2020) 20180115.
[26] D. Wellington, I. Mikaelian, L. Singer, Comparison of ketamine–xylazine and ketamine–dexmedetomidine anesthesia and intraperitoneal tolerance in rats, J. Am. Assoc. Lab. Anim. Sci. 52 (4) (2018) 481–487.
[27] N.W. Tietz, Clinical guide to laboratory tests, Clin. Guide Lab. Tests (1995) 1096–1996.
[28] C.A. Burtis, E.R. Ashwood, *Tietz textbook of clinical chemistry*. Amer Assn for Clinical Chemistry (1994).
[29] R.N. Ugbaja, E.I. Ugwor, D.I. Akinloye, V.O. Okereke, I.O. Meadows, A. O. Christianah, T.S. Lawal, Remedial effects of Aloe vera gel against diabetes-provoked disruptions in electrolyte homeostasis and ATPases activities in rats, Trace Elem. Electro 38 (3) (2021) 114.
[30] S. Junglee, L. Urban, H. Sallanon, F. Lopez-Lauri, Optimized assay for hydrogen peroxide determination in plant tissue using potassium iodide, Am. J. Anal. Chem. 5 (11) (2014) 730.
[31] X.X. Sreejayan, M.N.A. Rao, Nitric oxide scavenging by curcuminoids, J. Pharm. Pharmacol. 49 (1) (1997) 105–107.
[32] I. Rahman, A. Kode, S.K. Biswas, Assay for quantitative determination of glutathione and glutathione disulfide levels using enzymatic recycling method, Nat. Prot. 1 (6) (2006) 3159–3165.
[33] W.H. Habig, M.J. Pabst, G. Fleischner, Z. Gatmaitan, I.M. Arias, W.B. Jakoby, The identity of glutathione S-transferase B with ligandin, a major binding protein of liver, Proc. Nat. Acad. Sci. 71 (10) (1974) 3879–3882.
[34] S. Marklund, G. Marklund, Involvement of the superoxide anion radical in the autoxidation of pyrogallol and a convenient assay for superoxide dismutase, Eur. J. Biochem. 47 (3) (1974) 469–474.
[35] M.H. Hadwan, H.N. Abed, Data supporting the spectrophotometric method for the estimation of catalase activity, Data Brief. 6 (2016) 194–199.
[36] J.T. Rotruck, A.L. Pope, H.E. Ganther, A.B. Swanson, D.G. Hafeman, W. Hoekstra, Selenium: biochemical role as a component of glutathione peroxidase, Science 179 (4073) (1973) 588–590.
[37] J.A. Buege, S.D. Aust, Microsomal lipid peroxidation, Methods Enzym. 52 (1978) 302–310.
[38] C.A. Lygate, Maintaining energy provision in the heart: the creatine kinase system in ischaemia–reperfusion injury and chronic heart failure, Clin. Sci. 138 (8) (2024) 491–514.
[39] X. Chang, J. Liu, Y. Wang, X. Guan, R. Liu, Mitochondrial disorder and treatment of ischemic cardiomyopathy: potential and advantages of Chinese herbal medicine, Biomed. Pharmacother. 159 (2023) 114171.
[40] G. Ndrepepa, Aspartate aminotransferase and cardiovascular disease—a narrative review, J. Lab. Precis. Med 6 (2021) 6.
[41] S.A. Center, Interpretation of liver enzymes, in: Veter. Clin. North Amer.: Small Anim. Prac, 37, 2007, pp. 297–333.
[42] M. Haarhaus, G. Cianciolo, S. Barbuto, G. La Manna, L. Gasperoni, G. Tripepi, P. Magnusson, Alkaline phosphatase: an old friend as treatment target for cardiovascular and mineral bone disorders in chronic kidney disease, Nutrients 14 (10) (2022) 2124.
[43] J. Ouyang, H. Wang, J. Huang, The role of lactate in cardiovascular diseases, Cell Commun. Signal 21 (1) (2023) 317.
[44] N. Dwivedi, Y.D. Bhutia, V. Kumar, P. Yadav, P. Kushwaha, H. Swarnkar, S.J. S. Flora, Effects of combined exposure to dichlorvos and monocrotophos on blood and brain biochemical variables in rats, Hum. Exp. Toxicol. 29 (2) (2010) 121–129.
[45] R. Hussain, F. Ali, M.T. Javed, G. Jabeen, A. Ghaffar, I. Khan, M.T. Ghori, Clinico-hematological, serum biochemical, genotoxic and histopathological effects of trichlorfon in adult cockerels, Toxin Rev. 40 (4) (2021) 1206–1214.
[46] N. Teymouri, S. Mesbah, S.M.H. Navabian, D. Shekouh, M.M. Najafabadi, N. Norouzkhani, N. Deravi, ECG frequency changes in potassium disorders: a narrative review, Am. J. Cardiovasc. Dis. 12 (3) (2022) 112.
[47] R.H.G. Yamashita, V.N. Yamaki, N.N. Rabelo, L.C. Welling, E.G. Figueiredo, Acid-base and electrolyte disorders in neurocritical care, Neuro. Care Neurosurg. Princ. Appl. (2021) 373–390.
[48] L.A. Kleczkowski, A.U. Igamberdiev, Magnesium and cell energetics: at the junction of metabolism of adenylate and non-adenylate nucleotides, J. Plant Physiol. 280 (2023) 153901.
[49] W. Cárdenas-Aguazaco, A.L. Lara-Bertrand, L. Prieto-Abello, N. Barreto-López, B. Camacho, I. Silva-Cote, Exploring calcium-free alternatives in endochondral bone repair tested on In vivo trials-A review, Regen. Ther. 26 (2024) 145–160.
[50] A.M. Jafari-Nozad, A. Jafari, M. Aschner, T. Farkhondeh, S. Samarghandian, Curcumin combats against organophosphate pesticides toxicity: A review of the current evidence and molecular pathways, Curr. Med. Chem. 30 (20) (2023) 2312–2339.
[51] J. Lakshmi, K. Mukhopadhyay, P. Ramaswamy, S. Mahadevan, A systematic review on organophosphate pesticide and type II diabetes mellitus, Curr. Diabetes Rev. 16 (6) (2020) 586–597.

[52] A.L. Adedeji, A. Ogunniyi, D. Wusu, O.K. Afolabi, Dichlorvos exposure aggravates complications associated with diabetes in wistar rats, Int. J. Res. Stud. Biosci. 4 (7) (2016) 22–31.
[53] C.M.C. Andrés, J.M. Pérez de la Lastra, C.A. Juan, F.J. Plou, E. Pérez-Lebeña, The role of reactive species on innate immunity, Vaccines 10 (10) (2022) 1735.
[54] R.L. Benza, E. Grünig, P. Sandner, J.P. Stasch, G. Simonneau, The nitric oxide–soluble guanylate cyclase–cGMP pathway in pulmonary hypertension: from PDE5 to soluble guanylate cyclase, Eur. Resp. Rev. 33 (171) (2024) 230183.
[55] M. Kumar, S. Sharma, J. Kumar, S. Barik, S. Mazumder, Mitochondrial electron transport chain in macrophage reprogramming: potential role in antibacterial immune response, Curr. Res. Immunol. 5 (2024) 100077.
[56] K. Jomova, S.Y. Alomar, S.H. Alwasel, E. Nepovimova, K. Kuca, M. Valko, Several lines of antioxidant defense against oxidative stress: antioxidant enzymes, nanomaterials with multiple enzyme-mimicking activities, and low-molecular-weight antioxidants, Arch. Toxicol. 98 (5) (2024) 1323–1367.